UPE Self-Similarity in Gamma-Ray Bursts

A Comparative Study of Thermal Plus Nonthermal Continuum Prompt Emission

R. Ruffini, J. A. Rueda, **R. Moradi**, L. Li, L. M. Becerra, C. L. Bianco, M. Della Valle, C. L. Fryer, G. J. Mathews, M. T. Mirtorabi, Y. Aimuratov, F. Rastegarnia, C. Sigismondi, S. Zhang, S.-S. Xue, Y. Wang

ICRANet, Pescara · ICRA, Sapienza Università di Roma

The Sixth Zeldovich Meeting
ICRANet, Pescara, Italy — 13–17 July 2026

Outline

Gamma-ray bursts: the prompt keV–MeV emission

- Cosmological transients: a prompt γ-ray flash (ms–100 s), then X-ray/optical/radio afterglows.
- Prompt spectra fitted with the **Band** function or a cutoff power law (CPL).
- The short vs. long split is a useful first step, not a full description.
- Bright bursts are better read as a **sequence of episodes** (timing, spectrum, luminosity, multiwavelength).

This talk

Isolate one episode — the **ultrarelativistic prompt emission (UPE)**: a short, highly luminous keV–MeV interval whose spectrum is *thermal (blackbody) plus nonthermal* — and show this composite form is *empirically self-similar* across diverse GRBs.

[Band et al.1993); Meegan et al.2009); Piran2004); Ruffini et al.2021)]

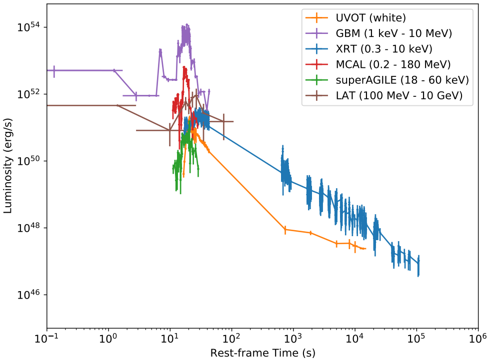

A GRB across wavelengths (GRB 220101A): prompt MeV/GeV, then X-ray and optical episodes.

A fifty-year thread: from "blackholic energy" to the UPE

1971–75
"blackholic energy" is extractable; QED pair creation around a BH proposed for GRBs

1998
the *dyadosphere*: overcritical-field shell where the $e^+e^-\gamma$ plasma is born

1999–2007
relativistic $e^+e^-\gamma$ plasma: thermalization, self-acceleration, transparency

2009–10
dyadoregion for rotating fields; Phys. Rep. review of the pair plasma

2016–2023
UPE identified & time-resolved: 151027A, 190114C, 180720B; self-similar hierarchy

2025
invariant dyadoregion of a Kerr BH in a B-field (Wald): pair initial conditions *& MHD acceleration*

This work
the UPE compared across eight GRBs

The 1970s idea

A black hole is *not* inert: it stores enormous **extractable electromagnetic and rotational energy** — up to $\sim 29\%$ (rotation) or 50% (charge) of Mc^2 (Christodoulou and Ruffini1971). Damour and Ruffini1975) showed that **QED vacuum polarization** around a Kerr–Newman BH creates e^+e^- pairs that tap it — the first BH pair-creation mechanism *proposed for gamma-ray bursts*.

[Christodoulou and Ruffini1971); Damour and Ruffini1975); Preparata et al.1998); Cherubini et al.2009); Ruffini et al.2010, 2018); Moradi et al.2021a); Rastegarnia et al.2022); Li et al.2023)]

Vacuum polarization and the critical field

- An electric field at the **critical (Schwinger) value**

$$E_c = \frac{m_e^2 c^3}{e\hbar} \simeq 1.3 \times 10^{16}\ \mathrm{V\ cm}^{-1}$$

  polarizes the vacuum and creates e^+e^- pairs.
- Theoretical line: Sauter; Dirac; **Euler–Heisenberg**; **Schwinger**; Breit–Wheeler.
- Not reachable in the lab — but **overcritical fields do occur** around compact objects.

Key point

The UPE thermal component is a candidate *astrophysical* manifestation of vacuum polarization.

[Heisenberg and Euler1936); Schwinger1951); review: Ruffini et al.2010)]

The black-hole realization and the effective charge

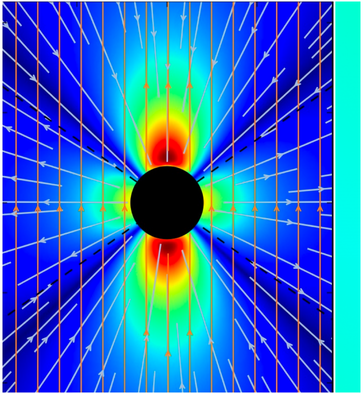

Kerr BH in an aligned field B_0: the *induced* electric field (colour) and field lines [Moradi et al. 2021].

- Damour and Ruffini1975): QED pair creation in **Kerr–Newman** geometries — energy extraction from an electromagnetic BH.
- Papapetrou–Wald: a Kerr BH in an external field B_0 *induces* an electric field that can exceed E_c.
- The **inner engine** replaces a net charge by an **effective charge**

$$Q_{\text{eff}} = \frac{2B_0 JG}{c^3},$$

so no net-charged BH is assumed (Ruffini et al.2019; Rueda and Ruffini2020). In the Wald solution the induced field is exactly that of an effective charge $|Q_{\text{eff}}| = 2JB_0$ (Cherubini et al.2025).

- Overcritical field $\Rightarrow$ pair creation in the **dyadoregion** (Cherubini et al.2009; Moradi et al.2021b).

[Damour and Ruffini1975); Cherubini et al.2009); Ruffini et al.2019); Rueda and Ruffini2020); Moradi et al.2021b); Cherubini et al.2025)]

The dyadosphere and the dyadoregion

- **Dyadosphere** (Preparata et al.1998): the shell around the BH where $E \geq E_c$; it fills with a thermalized, optically thick $e^+e^-\gamma$ plasma.
- Generalized to rotating fields as the **dyadoregion** of a rotating magnetic dipole (Cherubini et al.2009; Rueda et al.2026); its radius $r_d(\theta)$ and width $\Delta_d = r_d - R$ set the pair energy $\mathcal{E}_{e^+e^-}$.
- **New (2025):** an *invariant* characterization for a **Kerr BH in an external B-field** (Wald), giving the pairs' **initial conditions**; needs $B_0 \gtrsim$ few$\times 10^{14}$ G (Cherubini et al.2025).

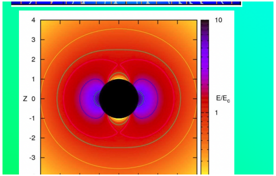

Dyadotorus E/E_c (Cherubini 2009).

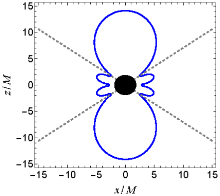

New: Kerr BH $+B$-field dyadoregion (Cherubini 2025).

Relations (Cherubini 2009, 2025): $\tilde{E}(r_d, \theta) = E_c$, $\bar{r}_d \approx (\xi\beta)^{1/2} |(3\cos^2\theta - 1)\cos\theta|^{1/2}$, $\mathcal{E} \propto B_0^{7/2} \sim 10^{52}$ erg ($\xi = a/M$, $\beta = B_0/B_c$).

[Preparata et al.1998); Cherubini et al.2009); Rueda et al.2026); Cherubini et al.2025)]

The optically thick $e^+e^-\gamma$ plasma: expansion and transparency

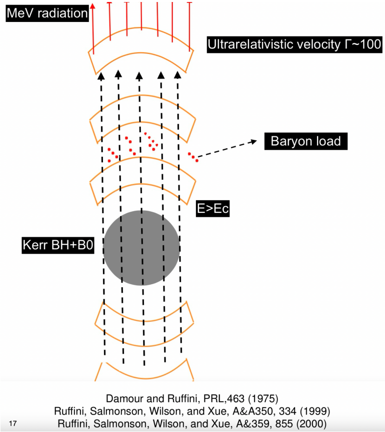

- The overcritical field creates an optically thick $e^+e^-\gamma$ plasma that **thermalizes** in $\sim 10^{-13}$ s (Aksenov et al.2007).
- **How it accelerates — two channels:**
  - (i) *Thermally driven* self-acceleration by its radiation pressure to $\Gamma \sim 1/\mathcal{B} \sim 100$ (Ruffini et al.1999, 2000).
  - (ii) **New (2025):** *magnetically driven* — pairs' pressure $\ll$ magnetic pressure, so ideal MHD converts **magnetic energy** $\rightarrow$ **pair kinetic energy** (Cherubini et al.2025).
- It carries a baryon load $\mathcal{B}$ and becomes **transparent**, releasing the **MeV blackbody**.
- **Why it iterates:** each discharge is *self-limiting* — the pairs screen the field and escape at transparency; the rotating engine then **rebuilds** the overcritical field, so the cycle **repeats**. Hence a rapid succession of elementary transparencies — the root of the observed *recurrence*.

overcritical field $\rightarrow$ $e^+e^-\gamma$ plasma $\rightarrow$ transparency $\rightarrow$ MeV BB $\rightarrow$ field rebuilt $\rightarrow$ *repeat*

[Damour and Ruffini1975); Ruffini et al.1999, 2000); Aksenov et al.2007); Cherubini et al.2025)]

Thermal components in GRBs are widely observed

- A blackbody-like component in prompt spectra has been reported by many groups:
  - Ryde2004, 2005): cooling thermal pulses; thermal emission may be common.
  - Guiriec et al.2011) (GRB 100724B), Axelsson et al.2012) (GRB 110721A): clear BB + nonthermal.
  - Broader samples: Yu et al.2019); Li2019); Li et al.2021).
- **Our question is more specific than "is there a BB?"**: does the same thermal+nonthermal form *recur under time subdivision*?

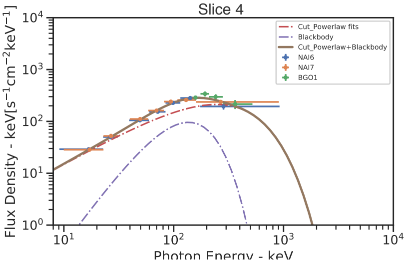

A thermal (blackbody) component superposed on a nonthermal continuum.

[Ryde and Svensson1999); Ryde2004, 2005); Guiriec et al.2011); Axelsson et al.2012); Yu et al.2019); Li2019); Li et al.2021)]

Other interpretations: the photospheric models

- **Photospheric emission**: the thermal radiation carried by the relativistic outflow, released where the flow becomes optically thin (the **photosphere**, $\tau_{\mathrm{T}} \approx 1$); sub-photospheric dissipation (shocks, reconnection) broadens the Planck spectrum toward Band-like.
  - Pe'er et al.2006); Pe'er2008): photospheric spectra & evolution.
  - Ryde and Pe'er2009): quiescent thermal component.
  - Beloborodov2010): collisional/dissipative photosphere.
- These reproduce a thermal component; recurrence under subdivision would *not* by itself distinguish them. What our reading adds is an **overcritical-field / pair-plasma origin** — the genuine discriminator (see later).

Our sharper question

Not "is there a blackbody?" — that is settled — but:

does the *same* BB+nonthermal form **recur under time subdivision**?

(We return to how this separates from a photosphere later.)

[Pe'er et al.2006); Pe'er2008); Ryde and Pe'er2009); Beloborodov2010)]

The UPE: an observational definition

UPE criterion (spectral & temporal only)

A short, highly luminous keV–MeV prompt interval whose spectrum **requires a thermal component** (one or several blackbodies) **together with a nonthermal continuum** (CPL or Band), and — when statistics allow — the same composite form **persists under subdivision**.

- *Not* defined by GeV emission, afterglow, supernova, or progenitor.
- Sample: GRBs **090510, 130427A, 160509A, 160625B, 180720B, 190114C, 220101A, 240825A**.
- Source data used only to convert to the rest frame ($kT_{\rm rf} = (1+z)kT_{\rm obs}$) and to set UPE boundaries.

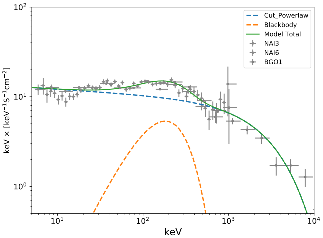

CPL + blackbody in a UPE interval (dashed: the BB component).

[This work; Ruffini et al.2016); Moradi et al.2021a); Rastegarnia et al.2022); Li et al.2023); Aimuratov et al.2023)]

Method and model comparison

- Time-resolved forward-folding through the detector responses (mainly Fermi-GBM; GBM/LAT for 090510).
- Model selection by information criteria (**DIC**, AIC, BIC); $|\Delta \mathrm{DIC}| > 10 =$ strong evidence.
- **Self-similarity test:** apply the same BB+nonthermal comparison at each successive time resolution (1, 2, 4, 8, 16 bins).
- Thermal fraction $\epsilon_{\mathrm{BB}} = F_{\mathrm{BB}}/F_{\mathrm{tot}}$ (or $E_{\mathrm{BB}}/E_{\mathrm{iso}}$).

$$\text{integrated interval} \rightarrow 2 \rightarrow 4 \rightarrow 8 \rightarrow 16 \text{ sub-intervals} \quad \text{(same spectral form retained)}$$

[Moradi et al.2021a); Rastegarnia et al.2022); Li et al.2023)]

Summary of the sample

GRB	UPE	z	$t_{\rm rf}$ (s)	Model	$E_{\rm iso}$ (erg)
090510	UPE	0.903	0.275–0.338	multi-BB+CPL	3.95×10^{52}
130427A	UPE	0.34	1.94–11.19	CPL+BB$^{\rm pile-up}$	$\sim 1.4 \times 10^{54}$
160509A	UPE	1.17	4.84–8.53	CPL+BB	5.40×10^{53}
160625B	UPE	1.406	77.72–87.70	CPL+BB	4.53×10^{54}
180720B	UPE I/II	0.654	4.84–6.05 / 9.07–10.89	CPL+BB	6.4×10^{52} / 1.6×10^{53}
190114C	UPE I/II	0.424	0.79–1.18 / 1.90–3.99	CPL+BB	1.0×10^{53} / 1.5×10^{53}
220101A	UPE I/II	4.61	15.15–16.04 / 18.72–19.61	CPL+BB	2.4×10^{53} / 4.6×10^{53}
240825A	UPE I/II	0.659	0.66–1.08 / 1.08–2.05	Band+BB	7.4×10^{52} / 9.0×10^{52}

- Rest-frame durations **0.063–9.98 s**; isotropic energies $\sim 4 \times 10^{52}$–4.53×10^{54} **erg** (excl. pile-up-limited 130427A).

[This work; sources cited per GRB below]

The dynamic range of the sample

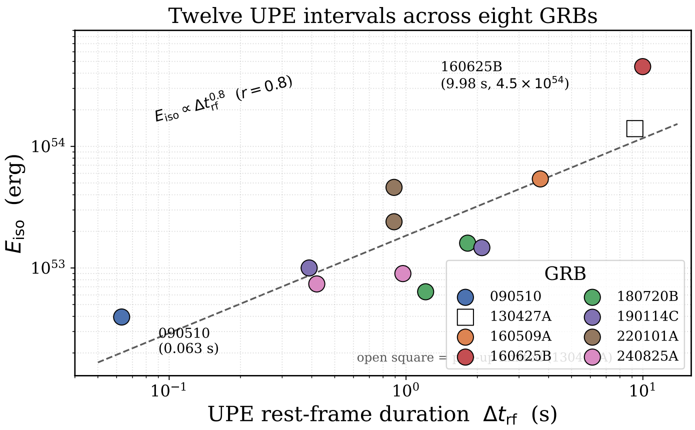

- Twelve UPE intervals span > 2 **decades** in duration (0.063–9.98 s) and energy ($\sim 4 \times 10^{52}$–4.5×10^{54} erg).
- $E_{\rm iso}$ grows with duration ($\propto \Delta t_{\rm rf}^{0.8}$, $r \approx 0.8$): the mean UPE luminosity is roughly **characteristic,** $\langle L \rangle = E_{\rm iso}/\Delta t_{\rm rf} \sim 10^{53}$ **erg s**$^{-1}$.
- From the *short* GRB 090510 to the most *energetic* 160625B — yet all share the **same** thermal-plus-nonthermal form.

[This work; values from the source analyses]

GRB 090510 — the short-GRB member

Role: the short-end limit — the hierarchy seen "edge-on".

not rebinnable · 63 ms integrated

- $z = 0.903$; UPE $t_{\rm rf} = 0.275$–0.338 s (0.063 s), $E_{\rm iso} = 3.95 \times 10^{52}$ erg.
- Integrated spectrum: nonthermal + **eight blackbodies**, $kT_{\rm obs} = 13$–1216 keV (25–2314 keV rest).
- Summed thermal fraction $\simeq 0.42$.
- Too short to rebin: multi-BB = *unresolved* analogue of the hierarchy seen in long GRBs.

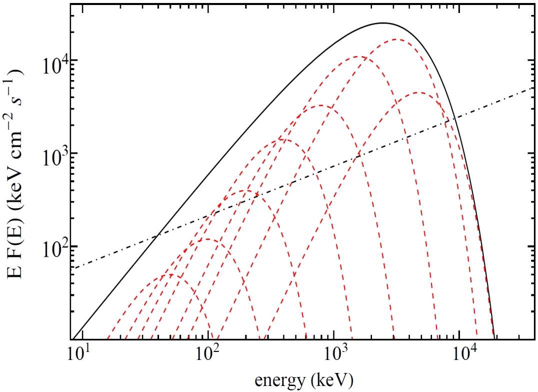

[Ruffini et al.2016); Ackermann et al.2010)]

GRB 190114C — two UPEs, hierarchy to 0.125 s

Role: the reference case — the deepest, cleanest hierarchy.

binned to 0.125 s · 16 bins

- $z \simeq 0.4245$; UPE I (0.79–1.18 s) $E_{\rm iso} = (1.00 \pm 0.11) \times 10^{53}$, $kT_{\rm rf} = 26.2$ keV.
- UPE II (1.90–3.99 s): CPL+BB, $\alpha = -0.71$, $E_c = 717.6$ keV, $kT_{\rm rf} = 159$ keV, $F_{\rm BB}/F_{\rm tot} = 0.20$.
- Same CPL+BB down to $\Delta t_{\rm rf} = 0.125$ s — the deepest hierarchy in the sample.

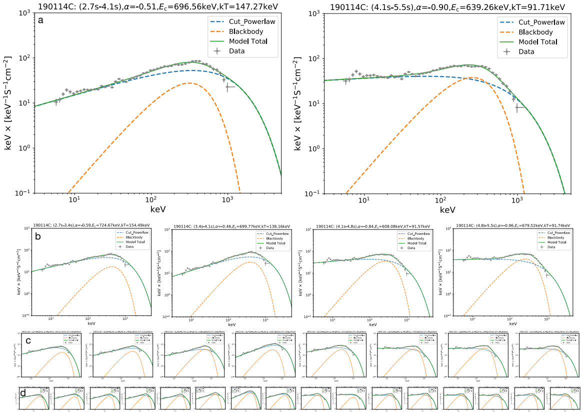

[Moradi et al.2021a); Aimuratov et al.2023)]

Role: reproducibility — an independent burst gives the *same* result.

binned to 0.11 s · 16 bins

- $z = 0.654$; UPE I (4.84–6.05 s) $E_{\rm iso} = (6.37 \pm 0.48) \times 10^{52}$, $kT_{\rm rf} = 83.2$ keV, four 0.30 s bins.
- UPE II (9.07–10.89 s): $\alpha = -1.06$, $E_c = 1502.5$ keV, $kT_{\rm rf} = 65.8$ keV; recovered down to 16 bins of $\simeq 0.11$ s.

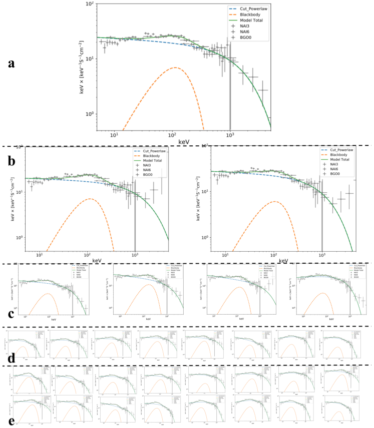

[Rastegarnia et al.2022)]

GRB 160625B & 160509A — twin 16-bin hierarchies

Role: the energetic anchor — it holds even at 4.5×10^{54} erg.

binned to 0.62 / 0.23 s · 16 bins each

160625B ($z = 1.406$): $E_{\rm iso} = 4.53 \times 10^{54}$ erg, $\Delta\mathrm{DIC} = -2840.2$, $\Delta t_{\rm rf} \simeq 0.62$ s

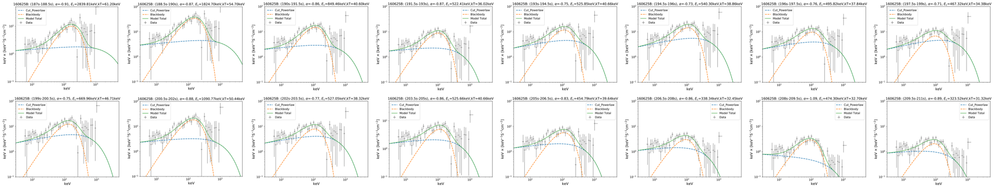

160509A ($z = 1.17$): $E_{\rm iso} = 5.40 \times 10^{53}$ erg, $\Delta\mathrm{DIC} = -633.8$, $\Delta t_{\rm rf} \simeq 0.23$ s

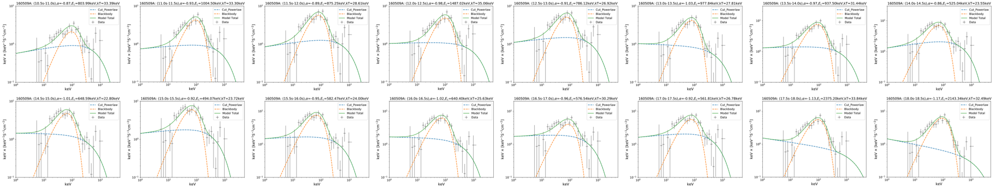

Each of the 16 sub-intervals (fifth iteration) is still best fit by CPL+BB.

130427A — the negative control

$z \simeq 0.34$; UPE 1.94–11.19 s, $E_{\rm iso} \sim 1.4 \times 10^{54}$ erg.

Severe Fermi-GBM **pile-up** $\Rightarrow$ the hierarchy test *cannot* be run: the claim is data-limited, not assumed — the test is real and *can* fail.

220101A — "New Year's", $z = 4.61$

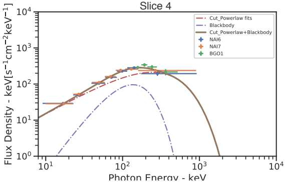

Two separated thermal pulses (slices 4 & 6), CPL+BB; $kT_{\rm rf} = 123,\ 181$ keV; $\epsilon_{\rm BB} \sim 0.30,\ 0.25$.

240825A — Band+BB, boundary

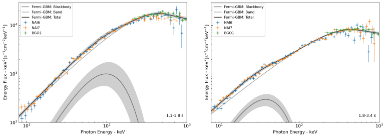

Two Band+BB peaks, $\Delta{\rm DIC} = 39.27,\ 49.77$; UPE I splits, stays Band+BB, $kT_{\rm rf}$ cools $63.7 \rightarrow 37.9$ keV.

All three show the thermal-plus-nonthermal UPE form, under different observational limitations.

[Ruffini et al.2015); Li et al.2023); Ruffini et al.2026b, submitted); Ruffini et al.2026a, submitted)]

The self-similarity test, visualized

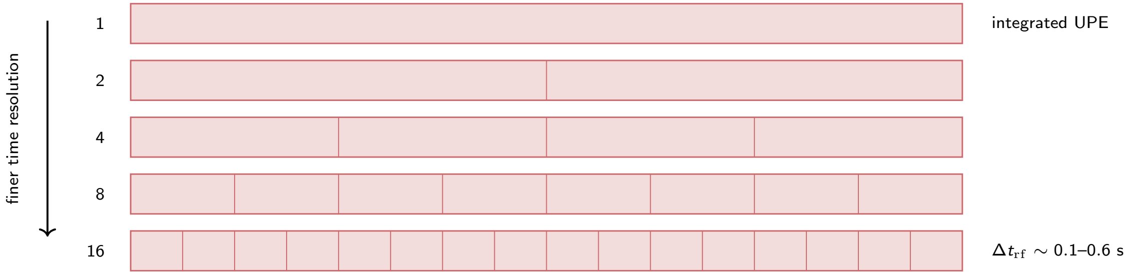

At *every* level, each bin is still best fit by the **same CPL/Band** + **blackbody** form ($|\Delta\mathrm{DIC}| \gg 10$).

[Moradi et al.2021a); Rastegarnia et al.2022); Li et al.2023)]

The self-similarity result

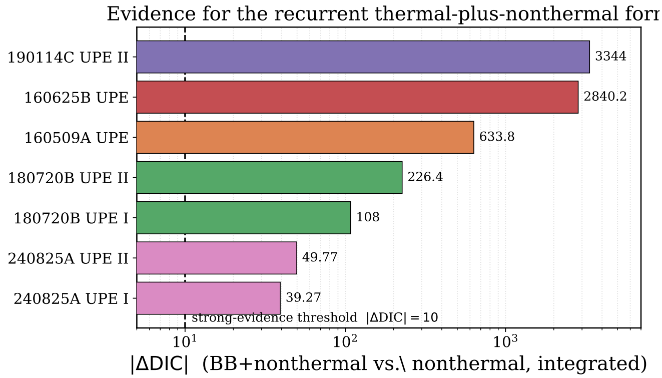

- The UPE is a *restricted* part of the prompt emission, requiring a thermal component on a nonthermal continuum.
- Under subdivision the **same composite form recurs** — best resolved (16-bin) in 190114C, 180720B, 160509A, 160625B (shortest bins 0.11–0.62 s).
- Adding the blackbody is favoured by $|\Delta \mathrm{DIC}| = 108$–3344 at *every* level — far above the threshold of 10.

[This work; Moradi et al.2021a); Rastegarnia et al.2022); Li et al.2023); Ruffini et al.2026a)]

Quantitative UPE evolution (fifth-iteration hierarchy)

GRB 160625B

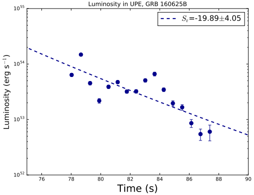

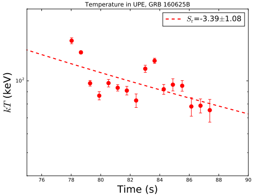

GRB 160509A

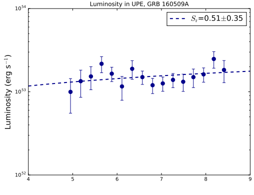

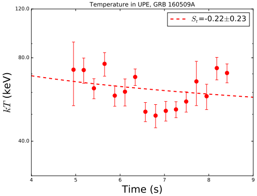

Luminosity and kT evolve across the UPE, while *each* short bin keeps the CPL+BB form.

[Li et al.2023)]

Temperatures, thermal fractions, luminosity scaling

- Integrated $kT_{\rm rf}$ span $\sim$ 16 keV (240825A II) to $\sim$ 181 keV (220101A II); 090510 alone runs tens of keV $\rightarrow$ MeV.
- Thermal fractions from the percent level (240825A) to tens of percent (090510, 190114C, 220101A).
- UPE luminosities follow simple power laws (indices *not* universal): e.g. -1.50 ± 0.30 (190114C), 0.36 ± 0.23 (180720B), 0.51 ± 0.35 (160509A).

$\Rightarrow$ Self-similarity concerns the **recurrence of the spectral form**, not a universal kT or $\epsilon_{\rm BB}$.

[Moradi et al.2021a); Rastegarnia et al.2022); Li et al.2023)]

Why not (just) a photosphere?

Photospheric models

- Thermal radiation released where the outflow becomes optically thin (the **photosphere**, $\tau_{\mathrm{T}} \approx 1$); sub-photospheric dissipation broadens it toward a Band-like spectrum.
- A well-developed, viable origin for the observed thermal component (Pe'er et al.2006; Pe'er2008; Beloborodov2010).

UPE (overcritical field)

- Blackbody from $e^+e^-\gamma$ pair-plasma transparency of an **overcritical field** ($E \geq E_c$).
- The BB+nonthermal form **persists down to the finest bins** — not an artifact of coarse time-integration (Burgess and Ryde2015).

What actually discriminates?

Persistence under subdivision shows the thermal component is *real* — but does not by itself exclude a photosphere. The genuine discriminator is whether the emission **requires an overcritical field**, a demand a photosphere does not make.

[Pe'er et al.2006); Pe'er2008); Beloborodov2010); Burgess and Ryde2015); this work]

The main message

The most luminous keV–MeV state of a GRB — the **UPE** — reappears with the **same thermal-plus-nonthermal form at every time scale**, across bursts of very different size and duration.

- **One recurrent state across diverse GRBs** — short (0.063 s) to the most energetic long (~ 10 s, 4.5×10^{54} erg). What is shared is the *radiation mechanism and spectral state*, even where the engines differ (merger-remnant NS, accreting companion NS, WD-born NS, or Kerr BH).
- **Each pulse is a rapid succession of events**, not one smooth release: the form persists to the shortest resolved bins (~ 0.1 s), consistent with an *inferred* $\sim 10^8$ successive pair-plasma transparencies (a model count, not a directly observed one) — the engine fires repeatedly.
- **A demanding constraint on the QED / pair-plasma reading**: the persistence rules out a coarse-binning artifact and is what an *overcritical field* predicts (Euler–Heisenberg/Schwinger) — a strong constraint every model must reproduce, though not, by itself, a unique proof over a photosphere.

[This work; Moradi et al.2021a); Li et al.2023); Rueda et al.2026)]

Time variability: how deep can we probe?

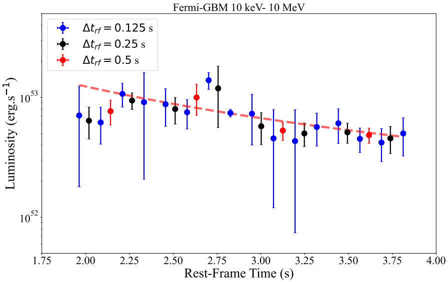

The UPE light curve, resolved on short timescales.

- The **minimum variability timescale** (MVT) — the shortest statistically significant variability — gauges the central-engine/emission-region activity (Golkhou and Butler2014; Golkhou et al.2015; MacLachlan et al.2013).
- Long GRBs: MVT $\sim$ 0.1–0.5 s (rest frame); short GRBs down to $\sim$ 10–30 ms.
- This is *comparable* to the spectral-subdivision floor ($\sim$ 0.1–0.6 s): the light curve **and** the spectra are both probed only to $\sim$ 0.1–0.5 s.
- Below that, the emission looks smooth and photon statistics run out — so the interpreted $\sim 10^8$ elementary pair-plasma events ($\sim$ns) are a **model extrapolation**, not an observed feature.

[Golkhou and Butler2014); Golkhou et al.2015); MacLachlan et al.2013); this work]

Transparency: reading the radiative state from the data

For one optically thick $e^+e^-\gamma$ pulse (E_0, $\epsilon_{\rm BB}$, $T_{\rm obs}$, shell width $\Delta_{\rm lab}$), transparency ($\tau_{\rm T} = 1$) gives:

$$\mathcal{B} \equiv \frac{M_{\rm b} c^2}{E_0} = \frac{1 - \epsilon_{\rm BB}}{\Gamma - 1}, \qquad R_{\rm tr} = \left(\frac{\sigma_T}{8\pi} \frac{\mathcal{B} E_0}{m_N c^2} \right)^{1/2},$$

$$\epsilon_{\rm BB} = \frac{a T_{\rm obs}^4}{16 \Gamma^2} \sigma_T \frac{\mathcal{B}}{m_N c^2} \Delta_{\rm lab}, \qquad \tau_{\rm T} \simeq \sigma_T \frac{\bar{Z} M_{\rm b}}{4\pi m_N R_{\rm tr}^2} = 1 \;\; (\bar{Z} = \tfrac{1}{2}).$$

- These fix Γ, $\mathcal{B}$, $R_{\rm tr}$ from the *observed* $E_0, T_{\rm obs}, \epsilon_{\rm BB}, \Delta_{\rm lab}$ — **no progenitor parameter** enters; the data constrain the **radiative state**, not the engine.
- The MeV blackbody escapes when the expanding shell reaches $\tau_{\rm T} = 1$; the ratio $E_{\rm BB}/E_0 = \epsilon_{\rm BB}$ sets the baryon load and Lorentz factor.
- **Persistence** of the same $(\epsilon_{\rm BB}, kT)$ under subdivision $\Rightarrow$ a *repetitive* transparency process on ever shorter timescales — the origin of self-similarity.

[Moradi et al.2021a); Rastegarnia et al.2022); Rueda et al.2026); Ruffini et al.1999, 2000); Aksenov et al.2007)]

Energetics: UPE vs. the other episodes

GRB	$E_{\rm UPE,iso}$ (erg)	$\sum E_{\rm non\text{-}UPE,iso}$ (erg)
090510	3.95×10^{52}	5.40×10^{52}
130427A	$\sim 1.4 \times 10^{54}$	1.10×10^{53}
160509A	5.40×10^{53}	4.24×10^{53}
160625B	4.53×10^{54}	4.46×10^{53}
180720B	2.24×10^{53}	1.98×10^{53}
190114C	2.47×10^{53}	7.27×10^{52}
220101A	7.0×10^{53}	3.89×10^{54}
240825A	1.64×10^{53}	5.09×10^{50}

- UPE exceeds the summed non-UPE energy in 130427A, 160509A, 160625B, 180720B, 190114C, 240825A (not in 090510, 220101A).
- Values are isotropic-equivalent, as reported by the source analyses.

[Rueda et al.2026); Li et al.2023); Rastegarnia et al.2022); Ruffini et al.2026b,a)]

A strong candidate within the BdHN framework

- **Fifty years of theory made this possible:** from the *charged* black hole (Christodoulou & Ruffini 1971) to the *effective charge* of a rotating BH in a magnetic field (the inner engine, 2019–2025) — the groundwork that now lets us reproduce the engine of the UPE in a **realistic, simulation-backed** way.
- Placement: the binary-driven hypernova (BdHN) — collapse of a $\mathrm{CO}_{\mathrm{core}}$ in a close binary; emission as a sequence of episodes.
- The UPE $e^+e^-\gamma$ plasma is created by an **overcritical field induced by a rotating, magnetized core** — the accreting NS approaching its critical mass *before* BH formation (or, equivalently, a Kerr BH in an external field).
- The rotational energy of the vortexing matter powers the UPE; successive transparencies give the self-similar blackbodies.

$\rightarrow$ The full theoretical development of this engine is the subject of the next talk, by J. A. Rueda.

[Ruffini et al.2026b, submitted); Rueda et al.2026); Moradi et al.2021a); Rastegarnia et al.2022)]

The BdHN binary: numerical simulation

- Progenitor: a CO core (~ 9–$10\,M_\odot$) with a companion NS ($\sim 2\,M_\odot$), orbital period a few minutes (BdHN I).
- 3D SPH (*SNSPH*): the CO-core collapse forms a νNS ($1.75\,M_\odot$) and ejects $\sim 7\,M_\odot$; the ejecta **hypercritically accrete** onto the νNS and the NS companion (masses and angular momenta evolved in full GR; eL3$\omega\rho$ EOS, critical mass $\approx 2.3\,M_\odot$).

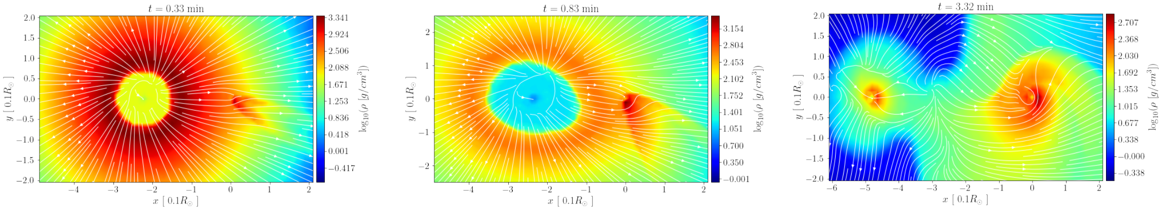

$t = 19.2$ s $\qquad$ $t = 49.8$ s: NS $\to$ critical mass $\qquad$ $t = 190.2$ s: post-collapse

Binary density maps; white curves = velocity field of the accreting SN ejecta.

[Ruffini et al.2026b, submitted); Becerra et al.2019, 2024); Aimuratov et al.2023)]

Vorticity of the accreting matter around the NS

- SN ejecta accreting on the companion NS form a high-angular-momentum **vortex**.
- Specific angular momentum $l \approx (2\text{–}3) \times 10^{17}$ cm^2 s^{-1}; bound mass $\sim 0.5\, M_\odot$.
- Total $L \sim (2\text{–}3) \times 10^{50}$ g cm^2 s^{-1}.
- l exceeds what a Kerr BH can hold ($a/M < 1$) $\Rightarrow$ this matter *cannot* enter the BH.

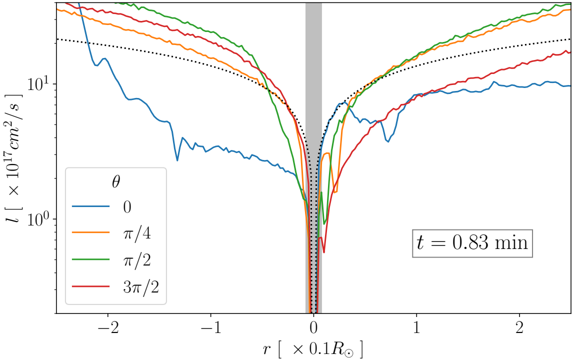

Specific angular momentum vs. radius at critical mass.

[Ruffini et al.2026b, submitted); simulations (Aimuratov et al.2023)]

Rotational energy → the UPE

- Angular velocity in the capture region $\Omega \approx 10^4$ rad s^{-1}.
- Rotational energy

$$E_{\rm rot} = \frac{1}{2}\Omega L \sim 10^{54} \text{ erg},$$

which **covers the UPE energetics**.

- This energy, unavailable to the BH, is released via the induced overcritical field.

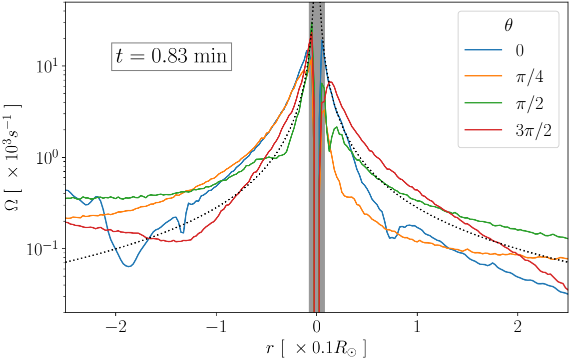

Angular velocity profiles of the bound, rotating matter.

[Ruffini et al.2026b, submitted)]

Dyadoregion of the rotating dipole and its shut-off

- The rotating magnetic field induces the overcritical electric field of an **effective charge**; pairs form in the dyadoregion (width $\Delta_d = r_d - R$).
- Exists only while $\Omega > \Omega_{\rm crit} \approx 7 \times 10^3$ rad s^{-1} (polar field $B_p \approx 1.1 \times 10^{14}$ G).
- As $\Omega \to \Omega_{\rm crit}$ the pair energy $\to 0$: the *time-varying* plasma initial conditions produce the **sequence of blackbodies** of the self-similar UPE.
- At the critical mass the BH forms, the field turns **undercritical**, pair creation ceases, and the GeV emission begins.

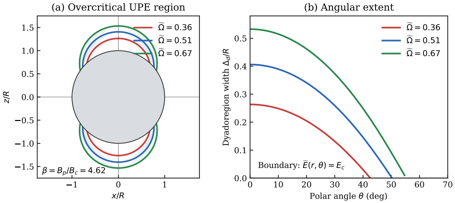

Dyadoregion boundary $r_d(\theta)$ and width around the rotating NS.

[Ruffini et al.2026b, submitted); Rueda et al.2026); GeV: Ruffini et al.2019); Rueda and Ruffini2020); Moradi et al.2021b); Rueda et al.2022)]

Transparency parameters and GRB 090510

- Applying the transparency relations to slices 4 & 6 gives per-event $\Gamma \sim 6$–10, $\mathcal{B} \sim 0.1$, $R_{\rm tr} \sim 10^{10}$ cm — *comparable* to 190114C and 180720B.
- $\sim 10^8$ transparency events build the observed self-similar UPE.
- **GRB 090510**: same mechanism, with the pair plasma from a rotating, magnetized **NS–NS merged core** before reaching the critical mass.

event	$kT_{\rm obs}$ (keV)	Γ	$R_{\rm tr}$ (10^{10} cm)
Slice 4	21.9	6.10	1.06
Slice 6	32.2	10.19	0.79

[Ruffini et al.2026b, submitted); Rueda et al.2026)]

The BdHN family and the GRB–SN connection

Seven episodes of a BdHN I

- SN-rise $\rightarrow$ νNS-rise $\rightarrow$ **UPE** $\rightarrow$ BH rise (GeV) $\rightarrow$ BH dynamics (cavity/flares) $\rightarrow$ X-ray afterglow $\rightarrow$ Ni decay.
- The **UPE is one episode** — the overcritical-field / BH-rise phase — not the whole burst.
- Sub-classes by orbital period: BdHN I ($\gtrsim 10^{52}$ erg, forms a BH), II, III.

The associated supernova

- A type Ic SN follows, powered by ^{56}Ni decay, seen $\sim$ 7–20 d later.
- 24 spectroscopic GRB–SNe: SN peak luminosity & time *independent* of the GRB energy (which spans $\sim$ 6 decades).
- The SN is a *separate episode* on its own timescale — kept apart from the keV–MeV UPE.

The UPE isolates the prompt-emission constraint within this multi-episode, binary picture.

[IGC: Rueda and Ruffini2012); Ruffini et al.2021); Aimuratov et al.2023)]

A new observational window: Insight-HXMT, GECAM, SVOM

Insight-HXMT

LE 1–15, ME 5–30,
HE 20–250 keV
HE/CsI GRB mode 0.2–3 MeV
25 μs timing; up to $\sim$1000s cm^2

X-rays to MeV; wide-field

GECAM

8 keV–$\sim$ 2 MeV
0.1 μs timestamps
25 detectors/spacecraft, all-sky

all-sky, high dynamic range

SVOM

ECLAIRs 4–150 keV; GRM to 5 MeV
20 μs timing
slews for afterglow

trigger $\rightarrow$ rapid follow-up

Why it matters

The decisive capability is not one detector but the **overlap**: broad energy coverage, high **dynamic range**, μs **timing**, and — for the brightest events — *unsaturated* spectra. This is what lets us push variability and spectral-hierarchy tests further.

[Instrument capabilities from the HXMT/GECAM/SVOM mission papers]

New trends in the prompt emission — three recent puzzles

GRB 240825A

(Wang et al. 2025)

Three spectral components in sequence: Band + thermal + a hard nonthermal component — and the thermal evidence *precedes* the hard/GeV one.

GRB 250706B/C

(Wang et al. 2026)

A pulse forest: $\geq$79 stochastic pulses (MVT $\sim$11 ms) under one smooth envelope — a *central-engine-dominated* signature.

GRB 221009A

(Moradi et al. 2026)

A moving MeV feature: a line drifting $\sim$37$\rightarrow$6 MeV — candidate relativistic ^{56}Ni decay lines.

Prompt emission shows **more components, more temporal structure, and more spectral features** than any single model naturally accommodates.

[Wang et al.2025, 2026); Moradi et al.2026)]

GRB 240825A: keV→GeV in a single burst

- Simultaneous **GECAM-B/C, Insight-HXMT, Fermi-GBM/LAT, Swift-BAT** coverage from keV to GeV ($z = 0.659$; *also a member of our UPE sample*).
- The integrated spectrum needs **Band** + **blackbody** + **cutoff-PL** ($E_{\rm p} \sim 502$ keV, $kT \sim 35$ keV, cutoff ~ 79 MeV).
- **The thermal evidence precedes the hard/GeV component** (transition $\sim$ 1.5–1.6 s, LAT turns on there).

⇒ Exactly the **UPE** → **inner-engine sequence**: MeV thermal first, GeV afterwards.

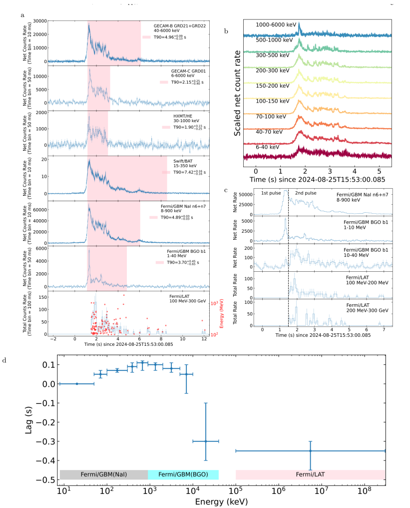

Figure 1. The lightcurve of GRB 240825A. (a) The lightcurve of GRB 240825A observed by different missions, along with the corresponding T_{90}. (b) The lightcurve of different energy ranges from keV to MeV observed by GECAM-B. It can be seen that the main pulse actually consists of a soft, slow component, as well as a hard and narrow component. (c) The lightcurve of different energy ranges from keV to GeV. The lightcurves of BGO and LAT are divided into two energy bands based on the dominant spectral components. The profile of the lightcurve in 10–40 MeV exhibits a bump shape, corresponding to the high-energy nonthermal

[Wang et al.2025)]

GRB 250706B/C: a pulse forest — a central-engine signature

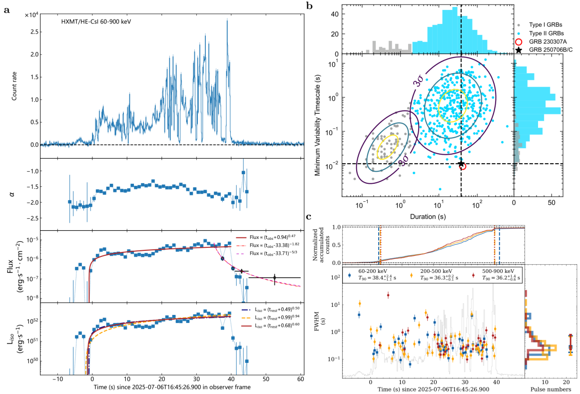

Figure 1. The light curve of GRB 250706B/C. (a) The time-resolved spectra and the peak-finding result. (b) The GRB 250706B/C in the T_{90}–MVT diagram. (c) The pulse width of GRB 250706B/C in three different energy ranges (i.e., 60–200 keV, 200–500 keV, and 500–900 keV) as well as the duration of the emission in these three energy ranges. There is no significant broadening or narrowing of both the subpulses and the overall prompt emission as a function of photon energy, suggesting a central-engine-dominated emission process rather than a dissipation-dominated emission process.

[Wang et al.2026)]

- Insight-HXMT/HE-CsI (60–900 keV): $\geq$**79 stochastic pulses**, MVT $\sim$11 ms, under a *simple* rising envelope ($F \propto (t - t_0)^{0.47}$); $z \simeq 0.942$.
- Long duration but a *short*-GRB variability timescale (outlier in the T_{90}–MVT plane).
- Pulse widths are **energy-independent** $\Rightarrow$ *central-engine-dominated*, not dissipation-dominated.

$\Rightarrow$ The **engine fires repeatedly** — the same “rapid succession of events” seen in the UPE; a fallback-accretion candidate.

GRB 221009A: the moving MeV line (GECAM-C)

- The brightest GRB recorded ($z = 0.151$, $E_{\rm iso} \sim 1.5 \times 10^{55}$ erg); GBM saturated at the peak, but **GECAM-C stayed unsaturated**.
- The spectrum needs **Band + a narrow emission line**: at 290–300 s, 12.28 ± 0.03 MeV, with a *tentative* 24.24 ± 0.12 MeV excess.
- The line **drifts systematically**, $\sim$37$\rightarrow$6 MeV over $\sim$250–350 s.

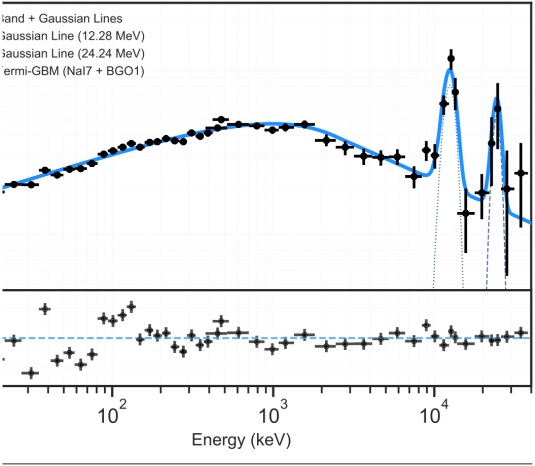

νF_ν: Band + line(s) at 12.28 & 24.24 MeV (Fermi-GBM) [Moradi et al. 2026].

[Moradi et al 2026; Zhang et al 2024; Ravasio et al 2024]

GRB 221009A: what is the moving line?

- **Pair annihilation:** the MeV line can be read as the 511 keV e^+e^- annihilation line, Doppler-boosted by the relativistic jet to MeV energies — one natural possibility.
- **Relativistic ^{56}Ni decay:** alternatively, the Doppler-boosted 158 keV line (^{56}Ni$\rightarrow$^{56}Co, 98.8% branch), with the higher excess matching the 270 keV branch.

$\Rightarrow$ The ^{56}Ni reading links the prompt/high-energy emission to **SN nucleosynthesis** — the SN episode of the BdHN picture. (Second feature: *candidate*, moderate significance.)

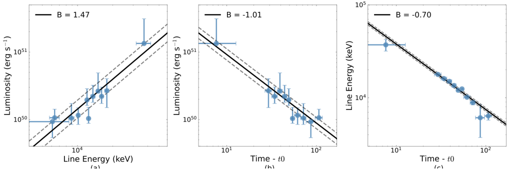

Line evolution: L–$E_{\rm line}$, L–t, $E_{\rm line}$–t power laws [Moradi et al. 2026].

[Moradi et al.2026); Zhang et al.2024); Ravasio et al.2024)]

What the new era means for the UPE and the inner engine

- The new missions deliver exactly what these tests need: **broad energy coverage**, μ**s timing**, and **unsaturated** spectra of the brightest bursts.
- That lets us (i) push **UPE self-similarity** to shorter timescales, (ii) resolve the **inner-engine GeV** phase, and (iii) catch rare features (moving lines, pulse forests) hidden at ordinary S/N.
- The three puzzles reinforce one message: prompt emission is **richer than any single model —** and our picture must confront the *full sequence* (UPE $\rightarrow$ inner engine $\rightarrow$ SN), not one feature.

$\Rightarrow$ The UPE self-similarity is the observational anchor; the new data are how we stress-test it.

[Wang et al.2025, 2026); Moradi et al.2026); this work]

Conclusions

- Across eight diverse GRBs (short, bright long, double-UPE, boundary), the UPE is a **recurrent thermal-plus-nonthermal MeV state**.
- Twelve UPE intervals; dynamic range **0.063–9.98 s** and $\sim 4 \times 10^{52}$–4.53×10^{54} **erg**.
- The defining property is **self-similarity**: the same BB+nonthermal form recurs under time subdivision ($|\Delta\mathrm{DIC}|$ up to 3344).
- In the pair-plasma reading, this points to **vacuum polarization in an overcritical field** (Euler–Heisenberg/Schwinger) and $e^+e^-\gamma$ transparency.
- A strong BdHN candidate: the **overcritical field of a rotating, magnetized core** (accreting NS near critical mass / Kerr BH), developed for GRB 220101A and applied to GRB 090510.

[This work]

Outlook

- Any physical model of the prompt emission must now reproduce **UPE self-similarity** and the **overcritical-field condition**.
- **Relation to photospheric models:** as discussed, a dissipative photosphere remains a viable source of the thermal component; the UPE goes further only through the *overcritical-field* requirement.
- **Insight-HXMT, GECAM and SVOM** — with their dynamic range, μs timing and unsaturated bright-burst spectra — will show whether UPE self-similarity is **universal**, and will resolve the inner-engine GeV phase and the rich new prompt-emission phenomena.

Thank you — and thanks to the organisers of the Sixth Zeldovich Meeting.

Ackermann, M., Asano, K., Atwood, W. B., Axelsson, M., Baldini, L., Ballet, J., Barbiellini, G., Baring, M. G., Bastieri, D., Bechtol, K., Bellazzini, R., Berenji, B., Bhat, P. N., Bissaldi, E., Blandford, R. D., Bloom, E. D., Bonamente, E., Borgland, A. W., Bouvier, A., Bregeon, J., Brez, A., Briggs, M. S., Brigida, M., Bruel, P., Buson, S., Caliandro, G. A., Cameron, R. A., Caraveo, P. A., Carrigan, S., Casandjian, J. M., Cecchi, C., Çelik, Ö., Charles, E., Chiang, J., Ciprini, S., Claus, R., Cohen-Tanugi, J., Connaughton, V., Conrad, J., Dermer, C. D., de Palma, F., Dingus, B. L., Silva, E. d. C. e., Drell, P. S., Dubois, R., Dumora, D., Farnier, C., Favuzzi, C., Fegan, S. J., Finke, J., Focke, W. B., Frailis, M., Fukazawa, Y., Fusco, P., Gargano, F., Gasparrini, D., Gehrels, N., Germani, S., Giglietto, N., Giordano, F., Glanzman, T., Godfrey, G., Granot, J., Grenier, I. A., Grondin, M.-H., Grove, J. E., Guiriec, S., Hadasch, D., Harding, A. K., Hays, E., Horan, D., Hughes, R. E., Jóhannesson, G., Johnson, W. N., Kamae, T., Katagiri, H., Kataoka, J., Kawai, N., Kippen, R. M., Knödlseder, J., Kocevski, D., Kouveliotou, C., Kuss, M., Lande, J., Latronico, L., Lemoine-Goumard, M., Llena Garde, M., Longo, F., Loparco, F., Lott, B., Lovellette, M. N., Lubrano, P., Makeev, A., Mazziotta, M. N., McEnery, J. E., McGlynn, S., Meegan, C., Mészáros, P., Michelson, P. F., Mitthumsiri, W., Mizuno, T., Moiseev, A. A., Monte, C., Monzani, M. E., Moretti, E., Morselli, A., Moskalenko, I. V., Murgia, S., Nakajima, H., Nakamori, T., Nolan, P. L., Norris, J. P., Nuss, E., Ohno, M., Ohsugi, T., Omodei, N., Orlando, E., Ormes, J. F., Ozaki, M., Paciesas, W. S., Paneque, D., Panetta, J. H., Parent, D., Pelassa, V., Pepe, M., Pesce-Rollins, M., Piron, F., Preece, R., Rainò, S., Rando, R., Razzano, M., Razzaque, S., Reimer, A., Ritz, S., Rodriguez, A. Y., Roth, M., Ryde, F., Sadrozinski, H. F.-W., Sander, A., Scargle, J. D., Schalk, T. L., Sgrò, C., Siskind, E. J., Smith, P. D., Spandre, G., Spinelli, P., Stamatikos, M., Stecker, F. W., Strickman, M. S., Suson, D. J., Tajima, H., Takahashi, H., Takahashi, T., Tanaka, T., Thayer, J. B., Thayer, J. G., Thompson, D. J., Tibaldo, L., Toma, K., Torres, D. F., Tosti, G., Tramacere, A., Uchiyama, Y., Uehara, T., Usher, T. L., van der Horst, A. J., Vasileiou, V., Vilchez, N., Vitale, V., von Kienlin, A., Waite, A. P., Wang, P., Wilson-Hodge, C., Winer, B. L., Wu, X. F., Yamazaki, R., Yang, Z., Ylinen, T., and Ziegler, M. (2010). Fermi Observations of GRB 090510: A Short-Hard Gamma-ray Burst with an Additional, Hard Power-law Component from 10 keV TO GeV Energies. *ApJ*, 716:1178–1190.

Aimuratov, Y., Becerra, L. M., Bianco, C. L., Cherubini, C., Della Valle, M., Filippi, S., Li, L., Moradi, R., Rastegarnia, F., Rueda, J. A., Ruffini, R., Sahakyan, N., Wang, Y., and Zhang, S. R. (2023). GRB-SN Association within the Binary-driven Hypernova Model. *ApJ*, 955(2):93.

Aksenov, A. G., Ruffini, R., and Vereshchagin, G. V. (2007). Thermalization of Nonequilibrium Electron-Positron-Photon Plasmas. *Physical Review Letters*, 99(12):125003.

Axelsson, M. et al. (2012). GRB 110721A: an extreme peak energy and signatures of the photosphere. *ApJL*, 757:L31.

Band, D., Matteson, J., Ford, L., Schaefer, B., Palmer, D., Teegarden, B., Cline, T., Briggs, M., Paciesas, W., Pendleton, G., Fishman, G., Kouveliotou, C., Meegan, C., Wilson, R., and Lestrade, P. (1993). BATSE observations of gamma-ray burst spectra. I - Spectral diversity. *ApJ*, 413:281–292.

Becerra, L., Ellinger, C. L., Fryer, C. L., Rueda, J. A., and Ruffini, R. (2019). SPH Simulations of the Induced Gravitational Collapse Scenario of Long Gamma-Ray Bursts Associated with Supernovae. *ApJ*, 871:14.

Becerra, L. M., Cipolletta, F., Fryer, C. L., Menezes, D. P., Providência, C., Rueda, J. A., and Ruffini, R. (2024). Occurrence of Gravitational Collapse in the Accreting Neutron Stars of Binary-driven Hypernovae. *ApJ*, 976(1):80.

Beloborodov, A. M. (2010). Collisional mechanism for gamma-ray burst emission. *MNRAS*, 407:1033–1047.

Burgess, J. M. and Ryde, F. (2015). Are GRB blackbodies an artefact of spectral evolution? *MNRAS*, 447(4):3087–3094.

Cherubini, C., Geralico, A., Rueda, H. J. A., and Ruffini, R. (2009). e^{-}-e^{+} pair creation by vacuum polarization around electromagnetic black holes. *Phys. Rev. D*, 79(12):124002.

References II

Cherubini, C., Moradi, R., Rueda, J. A., and Ruffini, R. (2025). Vacuum breakdown around a Kerr black hole surrounded by a magnetic field. *A&A*, 704:A69.

Christodoulou, D. and Ruffini, R. (1971). Reversible Transformations of a Charged Black Hole. *Phys. Rev. D*, 4:3552–3555.

Damour, T. and Ruffini, R. (1975). Quantum electrodynamical effects in Kerr-Newman geometries. *Phys. Rev. Lett.*, 35:463–466.

Golkhou, V. Z. and Butler, N. R. (2014). On the Minimum Variability Timescale of Gamma-Ray Bursts. *ApJ*, 787:90.

Golkhou, V. Z., Butler, N. R., and Littlejohns, O. M. (2015). The Energy Dependence of GRB Minimum Variability Timescales. *ApJ*, 811:93.

Guiriec, S. et al. (2011). Detection of a thermal spectral component in the prompt emission of GRB 100724B. *ApJL*, 727:L33.

Heisenberg, W. and Euler, H. (1936). Folgerungen aus der Diracschen Theorie des Positrons. *Zeitschrift fur Physik*, 98:714–732.

Li, L. (2019). Thermal components in gamma-ray bursts. i. how do they affect nonthermal spectral parameters? *The Astrophysical Journal Supplement Series*, 245(1):7.

Li, L., Rueda, J. A., Moradi, R., Wang, Y., Xue, S. S., and Ruffini, R. (2023). Self-similarities and Power Laws in the Time-resolved Spectra of GRB 190114C, GRB 130427A, GRB 160509A, and GRB 160625B. *ApJ*, 945(1):10.

Li, L., Ryde, F., Pe'er, A., Yu, H.-F., and Acuner, Z. (2021). Bayesian time-resolved spectroscopy of multipulse grbs: Variations of emission properties among pulses. *The Astrophysical Journal Supplement Series*, 254(2):35.

MacLachlan, G. A. et al. (2013). Minimum variability time-scales of long and short GRBs. *MNRAS*, 432:857–865.

Meegan, C., Lichti, G., Bhat, P. N., Bissaldi, E., Briggs, M. S., Connaughton, V., Diehl, R., Fishman, G., Greiner, J., Hoover, A. S., van der Horst, A. J., von Kienlin, A., Kippen, R. M., Kouveliotou, C., McBreen, S., Paciesas, W. S., Preece, R., Steinle, H., Wallace, M. S., Wilson, R. B., and Wilson-Hodge, C. (2009). The Fermi Gamma-ray Burst Monitor. *ApJ*, 702:791–804.

Moradi, R. et al. (2026). Relativistic ^{56}Ni decay lines in GRB 221009A. *Communications Physics*, 9:172.

Moradi, R., Rueda, J. A., Ruffini, R., Li, L., Bianco, C. L., Campion, S., Cherubini, C., Filippi, S., Wang, Y., and Xue, S. S. (2021a). Nature of the ultrarelativistic prompt emission phase of GRB 190114C. *Phys. Rev. D*, 104(6):063043.

Moradi, R., Rueda, J. A., Ruffini, R., and Wang, Y. (2021b). The newborn black hole in GRB 191014C proves that it is alive. *A&A*, 649:A75.

Pe'er, A. (2008). Temporal evolution of thermal emission from relativistically expanding plasma. *ApJ*, 682:463–473.

Pe'er, A., Mészáros, P., and Rees, M. J. (2006). The observable effects of a photospheric component on GRB and XRF prompt emission spectra. *ApJ*, 642:995–1003.

Piran, T. (2004). The physics of gamma-ray bursts. *Reviews of Modern Physics*, 76:1143–1210.

Preparata, G., Ruffini, R., and Xue, S.-S. (1998). The dyadosphere of black holes and gamma-ray bursts. *A&A*, 338:L87–L90.

References III

Rastegarnia, F., Moradi, R., Rueda, J. A., Ruffini, R., Li, L., Eslamzadeh, S., Wang, Y., and Xue, S. S. (2022). The structure of the ultrarelativistic prompt emission phase and the properties of the black hole in GRB 180720B. *European Physical Journal C*, 82(9):778.

Ravasio, M. E. et al. (2024). A mega-electron volt emission line in the spectrum of a gamma-ray burst. *Science*, 385:452–455.

Rueda, J. A. and Ruffini, R. (2012). On the Induced Gravitational Collapse of a Neutron Star to a Black Hole by a Type Ib/c Supernova. *ApJL*, 758:L7.

Rueda, J. A. and Ruffini, R. (2020). The blackholic quantum. *European Physical Journal C*, 80(4):300.

Rueda, J. A., Ruffini, R., and Kerr, R. P. (2022). Gravitomagnetic Interaction of a Kerr Black Hole with a Magnetic Field as the Source of the Jetted GeV Radiation of Gamma-Ray Bursts. *ApJ*, 929(1):56.

Rueda, J. A., Ruffini, R., and Wang, Y. (2026). Short GRB 090510: A magnetized neutron star binary merger leading to a black hole. *Journal of High Energy Astrophysics*, 50:100464.

Ruffini, R., Aimuratov, Y., Mirtorabi, M. T., Mohideen Malik, R. F., and Wang, Y. (2026a). GRB 240825A: Shortest BdHN I. *submitted to The Astrophysical Journal*.

Ruffini, R. et al. (2026b). GRB 220101A: A Most Energetic 10^{54} erg Long GRB Triggered by a Succession of Two Supernovae Seven Seconds Apart. *submitted to The Astrophysical Journal*.

Ruffini, R., Karlica, M., Sahakyan, N., Rueda, J. A., Wang, Y., Mathews, G. J., Bianco, C. L., and Muccino, M. (2018). A GRB Afterglow Model Consistent with Hypernova Observations. *ApJ*, 869(2):101.

Ruffini, R., Moradi, R., Rueda, J. A., Becerra, L., Bianco, C. L., Cherubini, C., Filippi, S., Chen, Y. C., Karlica, M., Sahakyan, N., Wang, Y., and Xue, S. S. (2019). On the GeV Emission of the Type I BdHN GRB 130427A. *ApJ*, 886(2):82.

Ruffini, R., Moradi, R., Rueda, J. A., Li, L., Sahakyan, N., Chen, Y. C., Wang, Y., Aimuratov, Y., Becerra, L., Bianco, C. L., Cherubini, C., Filippi, S., Karlica, M., Mathews, G. J., Muccino, M., Pisani, G. B., and Xue, S. S. (2021). The morphology of the X-ray afterglows and of the jetted GeV emission in long GRBs. *MNRAS*, 504(4):5301–5326.

Ruffini, R., Muccino, M., Aimuratov, Y., Bianco, C. L., Cherubini, C., Enderli, M., Kovacevic, M., Moradi, R., Penacchioni, A. V., Pisani, G. B., Rueda, J. A., and Wang, Y. (2016). GRB 090510: A Genuine Short GRB from a Binary Neutron Star Coalescing into a Kerr-Newman Black Hole. *ApJ*, 831:178.

Ruffini, R., Salmonson, J. D., Wilson, J. R., and Xue, S. S. (1999). On the pair electromagnetic pulse of a black hole with electromagnetic structure. *A&A*, 350:334–343.

Ruffini, R., Salmonson, J. D., Wilson, J. R., and Xue, S.-S. (2000). On the pair-electromagnetic pulse from an electromagnetic black hole surrounded by a baryonic remnant. *A&A*, 359:855–864.

Ruffini, R., Vereshchagin, G., and Xue, S. (2010). Electron-positron pairs in physics and astrophysics: From heavy nuclei to black holes. *Phys. Rep.*, 487:1–140.

Ruffini, R., Wang, Y., Enderli, M., Muccino, M., Kovacevic, M., Bianco, C. L., Penacchioni, A. V., Pisani, G. B., and Rueda, J. A. (2015). GRB 130427A and SN 2013cq: A Multi-wavelength Analysis of An Induced Gravitational Collapse Event. *ApJ*, 798:10.

Ryde, F. (2004). The Cooling Behavior of Thermal Pulses in Gamma-Ray Bursts. *ApJ*, 614:827.

Ryde, F. (2005). Is Thermal Emission in Gamma-Ray Bursts Ubiquitous? *ApJL*, 625:L95.

Ryde, F. and Pe'er, A. (2009). Quiescent thermal emission from the early phase of gamma-ray bursts. *ApJ*, 702:1211–1229.

Ryde, F. and Svensson, R. (1999). On the Shape of Pulse Spectra in Gamma-Ray Bursts. *ApJ*, 512:693–698.

Schwinger, J. (1951). On Gauge Invariance and Vacuum Polarization. *Physical Review*, 82:664–679.

Wang, C.-W. et al. (2025). Evolution of the Three Spectral Components in the Prompt Emission of GRB 240825A. *ApJL*, 985:L30.

Wang, C.-W. et al. (2026). GRB 250706B/C: Insight-HXMT Discovery of a High-luminosity Burst as a Candidate for Fallback-regulated Accretion in the Prompt Emission. *ApJL*, 1004:L44.

Yu, H.-F., Dereli-Bégué, H., and Ryde, F. (2019). Bayesian Time-resolved Spectroscopy of GRB Pulses. *ApJ*, 886(1):20.

Zhang, Y.-Q. et al. (2024). Observation of spectral lines in the exceptional GRB 221009A. *Science China Physics, Mechanics & Astronomy*, 67:289511.